THE JOURNAL OF PHYSICAL CHEMISTRY B

Article

pubs.acs.org/JPCB

Plasticization of Poly(vinylpyrrolidone) Thin Films under Ambient Humidity: Insight from Single-Molecule Tracer Diffusion Dynamics

Sukanya Bhattacharya,[†] Dharmendar Kumar Sharma,[†] Saumya Saurabh,[†,¶] Suman De,[†] Anirban Sain,[‡] Amitabha Nandi,[§,⊥] and Arindam Chowdhury*[,†]

[†]Department of Chemistry and [‡]Department of Physics, Indian Institute of Technology Bombay, Powai, Mumbai 400076, India

[§]Department of Molecular, Cellular and Developmental Biology, Yale University, New Haven, Connecticut 06520, United States

Supporting Information

ABSTRACT: Studies on diffusion dynamics of single molecules (SMs) have been useful in revealing inhomogeneity of polymer thin films near and above the glass-transition temperature (T_g). However, despite several applications of polymer thin films where exposure to solvent (or vapor) is common, the effect of absorbed solvent molecules on local morphology and rigidity of polymer matrices is yet to be explored in detail. High-T_g hydrophilic polymers such as poly(vinylpyrrolidone) (PVP) are used as pharmaceutical coatings for drug release in aqueous medium, as they readily absorb moisture, which results in effective lowering of the T_g and thereby leads to plasticization. The effect of moisture absorption on swelling and softening of PVP thin films was investigated by visualizing the diffusion dynamics of rhodamine 6G (Rh6G) tracer molecules at various ambient relative humidities (RH). Wide-field epifluorescence microscopy, in conjunction with high-resolution SM tracking, was used to monitor the spatiotemporal evolution of individual tracers under varied moisture contents of the matrix. In the absence of atmospheric moisture, Rh6G molecules in dry PVP films are translationally inactive, suggestive of rigid local environments. Under low moisture contents (RH 30−50%), translational mobility remains arrested but rotational motion is augmented, indicating slight swelling of the polymer network which marks the onset of plasticization. The translational mobility of Rh6G was found to be triggered only at a threshold ambient RH, beyond which a large proportion of tracers exhibit extensive diffusion dynamics. Interestingly, SM tracking data at higher moisture contents of the film (RH ≥ 60%) reveal that the distributions of dynamic parameters (such as diffusivity) are remarkably broad, spanning several orders of magnitude. Furthermore, Rh6G molecules display a wide variety of translational motion even at a fixed ambient RH, clearly pointing out the extremely inhomogeneous environment of plasticized PVP network. Intriguingly, it is observed that a majority of tracers undergo anomalous subdiffusion even under high moisture contents of the matrix. Analyses of SM trajectories using velocity autocorrelation function reveal that subdiffusive behaviors of Rh6G are likely to originate from fractional Brownian motion, a signature of tracer dynamics in viscoelastic medium.

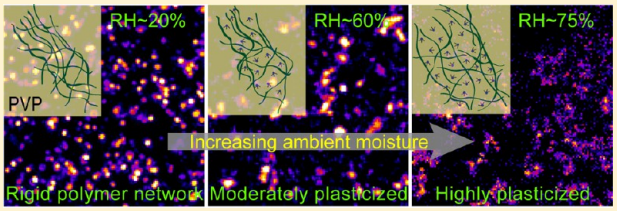

1. INTRODUCTION

Physical properties of polymer thin films differ substantially from that of bulk materials, and in particular, structure dynamics of polymer thin films are not completely understood.[1−3] In contrast to simple liquids, polymer thin films have been shown to exhibit nonidentical and nonexponential structural relaxation, which suggests the existence of static as well as dynamic inhomogeneity.[4−6] Depending on the state and thickness of polymer films and preparation methods, as well as the temperature of measurements, the extent of inhomogeneity can vary considerably, the understanding of which has become a focus of attention.[3,7,8] Single-molecule fluorescence microscopy (SMFM) has emerged to be an important tool to investigate inhomogeneity in such complex systems due to its ability to probe the unique local environment in the vicinity of individual molecules, via either changes in electronic properties or spatiotemporal behaviors.[9,10] Moreover, spectroscopy and dynamics of single molecules (SMs) can provide information on the distribution of measured properties which are obscured in ensemble measurements, essential in the context of heterogeneity.[9−11] For instance, explicit structural and chemical interactions within polymeric thin films have been investigated at the nanoscale using the dynamics of individual molecules,[10,12−18] while information about dynamic inhomogeneity and polymer segmental motion has been revealed by SM radiative lifetime measurements[19] as well as via rotational diffusion measurements.[20,21] Further, the rotational mobility of SMs in polymer matrices exhibits highly heterogeneous dynamics near the glass transition temperature (T_g).[13,15,22] On the other hand, translational diffusion of SMs in polymer thin films has been realized either for measurements performed above the bulk T_g[21,23] or under certain situations such as probe molecules located close to the polymer−air interface[23,24] and the presence of residual solvents in the thin-film matrix.[25]

Received: February 18, 2013
Revised: May 20, 2013
Published: June 4, 2013

   dx.doi.org/10.1021/jp401704e | J. Phys. Chem. B 2013, 117, 7771−7782

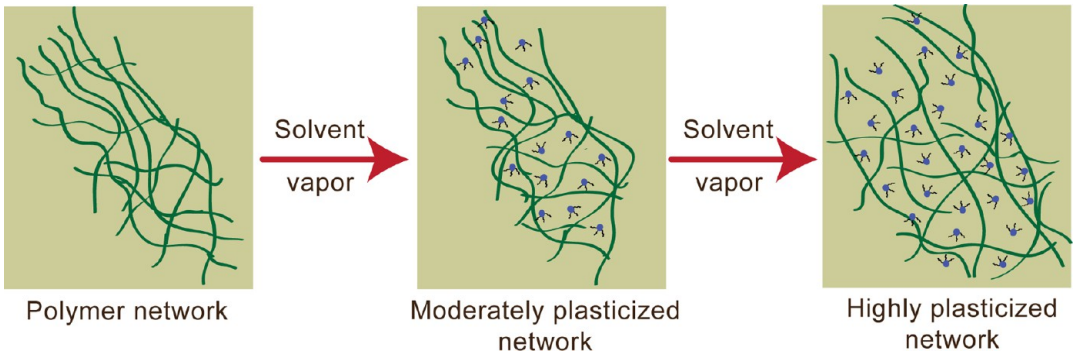

Figure 1. Schematic depiction of plasticization: solvent (vapor) absorption mediated swelling of the polymer network results in an increase in the effective free volume.

Under ambient conditions, the translational mobility of SMs in high-T_g polymer films is arrested considerably[12] or their dynamics is extremely slow,[26] likely due to rigidity of the matrix and the hindrance offered by the surrounding polymer network (i.e., the cavity) where the tracers are embedded.

So far, most SM diffusion studies in various polymer films have primarily focused on understanding tracer dynamics upon variation of film thickness (tens to hundreds of nanometers) and temperature (near or above the T_g), and related the variability in dynamic parameters to heterogeneity of the thin-film matrix.[23,24] Interestingly, there is a dearth of literature on how translational mobility of SMs in polymer thin films is affected in the presence of absorbed solvent,[14,27] even though it is well-known that certain solvents (or solvent vapor) can spontaneously percolate into the matrix and alter the morphology of the polymer network.[27,28] Solvent absorption induced softening and swelling of polymers, referred to as "plasticization", arises from lowering of intra-/intermolecular forces between densely packed polymer chains.[28,29] Penetration of such "good" solvents leads to an increase in the free volume of the polymer matrix (Figure 1), and depending on extent of solvent absorption, the T_g of the polymer is lowered considerably (often close to or below 300 K).[30] Therefore, plasticization effectively transforms a high-T_g polymer into a rubbery state. As a consequence, plasticizers (solvents or other small molecule additives) can severely alter several physical properties such as tensile strength, friction/lubrication, brittleness, and adhesion.[30,31] Since high-T_g polymer thin films have a wide variety of applications in nanoelectronic sensors/devices,[32] anticorrosion coatings,[33] fuel cells,[34] and controlled drug delivery[35] where exposure to solvent (or vapor) is quite common, it is extremely important to understand how the presence of different amounts of absorbed solvents influences the network morphology and thereby its viscoelastic behaviors. Besides, it is of fundamental interest to gain insight on how a polymer thin film is plasticized at the microscopic level and the extent of inhomogeneity during the process. These can be addressed by investigating the mobility of SMs in polymer thin films plasticized to different extents.

The choice of polymer and the solvent (or solvent vapor) is crucial to trigger tracer diffusion in solvent-absorbed polymer films because the extent of swelling (i.e., increase in free volume) depends on favorable interactions between the polymer film under investigation and the solvent used as absorbate.[30] For instance, it has been shown that SM probes located in hydrophobic poly(methyl methacrylate) (PMMA) thin films did not display any spatiotemporal changes even at saturation conditions of ambient humidity.[14] In contrast, for hydrophilic poly(vinyl alcohol) (PVA) films, both rotational and translational dynamics of probes occur even at lower atmospheric moisture contents.[14] While there are almost no reports on how different amounts of organic solvent vapor (like chloroform and toluene) affect the dynamics of SMs in hydrophobic polymer films,[27] it is known that low dielectric solvents can effectively swell low-polarity polymers networks to allow for diffusion of small molecules.[28,36] On the other hand, the chemical nature and size of fluorescent probes are also important for investigating dynamic behavior of tracers. Even though semiconductor nanocrystals (quantum dots) are ideal for single-particle tracking measurements in solution,[37] their large dimensions (typically >∼5 nm) render these unsuitable to probe diffusion dynamics within polymer matrices; slight swelling of the polymer network upon absorption of low to moderate amounts of solvent might induce rotational mobility of quantum dots, but their translational motion is likely to be inhibited or localized within few nanometers. On the contrary, despite photobleaching issues, smaller (∼1−2 nm) fluorescent molecules serve as ideal tracers to investigate diffusion dynamics in polymer films due to high sensitivity of spatiotemporal behaviors (as well as electronic properties) upon changes in rigidity, polarity, and viscosity of the local environment.[38,39]

Previously, Hou et al. investigated the effect of ambient RH on the changes in fluorescence signal and rotational/translational mobility of individual water-soluble fluorophores, located on and in hydrophilic (PVA) polymer thin films.[14] They have shown that fluorescence intermittency (blinking) and survival times (bleaching time) of SM probes were affected dramatically with increase in ambient RH. In addition, under moderate ambient RH of ∼60%, SMs undergo faster reorientation and their translational motion is initiated, suggesting that water vapor can effectively penetrate into the PVA matrix and lower its rigidity. However, due to low time resolution of the experiments, long time trajectories needed for evaluating diffusivities could not be obtained. Further, a lack of statistically relevant data sets made it impossible to provide distribution of diffusion coefficients and variability of dynamic behaviors, which are essential to understand inhomogeneity of the polymer network.

We chose poly(vinylpyrrolidone) (PVP), a high-T_g (∼428 K) amorphous polymer, which is often used as coatings on pharmaceuticals due to its water solubility and biocompatibility.[40,41] Moreover, thin films of PVP have important applications for controlled drug delivery.[35,41] PVP serves as a

dx.doi.org/10.1021/jp401704e | J. Phys. Chem. B 2013, 117, 7771−7782

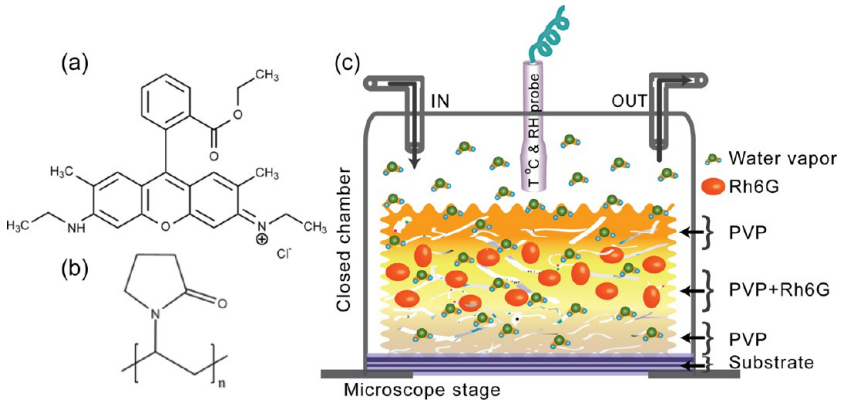

Figure 2. Structures of (a) rhodamine 6G (Rh6G) and (b) poly(vinylpyrrolidone) (PVP). (c) Schematic of the working set up showing the thin-film structure with Rh6G embedded inside PVP matrix, within a RH-controlled enclosed chamber mounted on a microscope stage.

model system to study plasticization because it is well-known that this polymer readily absorbs moisture from the atmosphere (by up to ∼40% of its weight) and the extent of water uptake increases continuously with ambient RH.[42,43] As a consequence, there is a dramatic lowering of the bulk T_g of PVP; for instance, ∼25% moisture absorption (at ∼70% RH) leads to a T_g of ∼300 K.[42−44] For PVP thin films, however, the T_g is expected to be lowered even further under similar conditions. Interestingly, how the morphology and viscoelastic properties of PVP thin-film matrices are altered locally in the presence of different amounts of moisture has not been investigated as of yet. Moreover, from the standpoint of diffusivity of small drug molecules encapsulated in PVP films, it is relevant to find the variability in dynamic behaviors of entrapped tracer molecules similar in dimensions to pharmaceutical drugs during the course of plasticization.

In this work, we utilize SMFM to visualize the dynamics of individual tracer molecules in PVP thin films under varied moisture contents of the matrix, achieved by incorporating rhodamine 6G (Rh6G) probe molecules in the thin film and following their spatiotemporal evolution under various ambient RH. Wide-field epifluorescence microscopy allowed for simultaneous detection of a large number of individual molecules and monitoring their spatiotemporal behaviors. Single-molecule tracking (SMT) was used to determine the spatial locations of the probes at subpixel resolution and investigate the variability in their dynamic behaviors at three different RH regimes. While our results indicate that the PVP matrix is extremely rigid under dry conditions, we find that plasticization in initiated at quite low amounts of moisture content in the matrix. However, translational motion of SMs is detectable only above a certain level of ambient RH, beyond which tracers display a wide range of dynamic behaviors reflecting the variations in local morphology and viscosity. Intriguingly, it is observed that a significant population of SMs undergoes subdiffusive motion while they navigate through the plasticized polymer network, reminiscent of tracers in cellular environments. Analysis of SM trajectories using velocity autocorrelation function provides a mechanistic insight on subdiffusion of tracers in plasticized PVP thin films.

2. MATERIALS AND METHODS

2.1. Materials. Poly(vinylpyrrolidone) (MW 40 000, Sigma Aldrich) was used as received. Rhodamine 6G (Radiant Dyes, Germany) was used as the fluorescent probe. Glass coverslips (No. 1, Corning, USA) were used as the substrate to deposit the polymer.

2.2. Sample Preparation. Glass coverslips were first sonicated for 15 min in Piranha solution and then in 2 M NaOH, followed by washing several times with Milli Q water and eventually methanol. After blowing N_2 gas to dry, the coverslips were burnt in an oxidizing flame to remove any residual fluorescent impurity. To ensure that majority of the rhodamine 6G (Rh6G) probes are located inside the polymer network and not near the polymer−air or substrate−polymer interface, thin films of ∼200 nm thickness were prepared by a method previously employed by Liu et al.[45] The process involves spin coating (2000 rpm, 1 min) (i) one drop of 2 mg/mL PVP solution in Milli-Q water on freshly cleaned coverslips, followed by (ii) one drop of ∼0.3 nM solution (one drop) of Rh6G premixed with PVP (2 mg/mL), and eventually (iii) one more drop of PVP-only solution on top of the preformed films. To prepare thicker (∼500 nm) films, the last step was repeated 7−8 times on top of the preformed (PVP/PVP-Rh6G/PVP) films. Additionally, Rh6G (without PVP) solution was spin-cast on preformed films cast from three drops PVP solution to generate thin-film samples where tracer molecules reside near the polymer−air interface.[13,14] The thickness of films was determined using both atomic force microscopy and ellipsometry and it was found that addition of each drop of PVP or PVP/Rh6G solution resulted in the film thickness increase of ∼60−70 nm. To remove the residual solvent and generate a relaxed polymer film, the samples were annealed ∼120 °C for 2 h under evacuated conditions. The annealed thin film was placed inside a home-built enclosed chamber mounted over the microscope stage and subjected to ambient moisture (illustrated in Figure 2c). The humidity was regulated by controlling a (continuous) flow of argon gas through water into the enclosed chamber, and was monitored using a RH probe suspended a few millimeters above the sample. The RH levels were maintained within ±2% of a desired value for 30 min before data collection and kept constant during measurements.

2.3. Single-Molecule Fluorescence Microscopy. A home-built laser epifluorescence setup based on an inverted microscope (Nikon TE2000) was used to perform SM imaging measurements and monitor their spatiotemporal behaviors. A 532 nm cw DPSS laser (LaserGlow, 50 mW) light (circularly polarized using $\lambda/4$ plate) was focused onto the back focal plane of a 60× 1.49 NA oil immersion objective (Nikon, Apo Plan TIRF) to illuminate a circular area (∼30 μm diameter) of the sample. The excitation power was controlled using ND

dx.doi.org/10.1021/jp401704e | J. Phys. Chem. B 2013, 117, 7771−7782

filters and maintained at ~2 mW measured before the objective. The emission from sample was collected using the same objective lens, passed through a dichroic mirror (Semrock, Di01-R532) and sharp-cutoff long-pass filter (Semrock, LP03-532RU). The emission was guided through relay lenses and imaged using a cooled (−25 °C) interline CCD camera (DVC-1412AM). To detect spatiotemporal changes, movies (16-bit image format) were collected over 30−60 s at 10 Hz; however, exposure time of 100 ms provided higher signal to background ratio (SBR). The microscope configuration was switched to through-the-objective total internal reflection fluorescence (TIRF) microscopy mode to detect non-Gaussian emission patterns (under focused conditions) arising from vertically aligned molecules (perpendicular to the sample plane).[46] To obtain the 3D orientation of transition dipoles of individual probes at intermediate RH levels, defocused imaging was performed in epifluorescence configuration[10,47,48] with extent of defocusing kept to ~1 μm. Due to relatively weak intensities of non-Gaussian/defocused emission patterns, a higher excitation power (5 mW) and exposure time (1 s) were used. It was verified that we detect Rh6G molecules by collecting their emission spectra under dry conditions (i.e., for immobile spots) using spectrally resolved imaging following refs 49 and 50. In addition to polarized light emission from individual diffraction limited spots, their fluorescence intermittency (blinking) and single-step photobleaching revealed that single Rh6G molecules were being detected. All measurements were carried out at 295 K.

2.4. Image Analyses and Representation. The CCD camera software (DVC View) was used to collect movies following which background subtraction and smoothing were performed using ImageJ (NIH). To represent the dynamic information of SM spatial locations contained in a movie onto a single image, the *maximum projection* image of the movie (over 10 s) was generated (using ImageJ), where individual pixels in the projection image display the maximum value that was recorded in the corresponding pixels (for individual frames) over a fixed number of acquired frames.[51] The data from a movie containing molecules with diverse diffusivities is presented in this fashion instead of simple overlay (i.e., average) due to the following reason. Time average of individual frames of a movie containing dynamic as well as stationary spots inadvertently overemphasizes stationary molecules and background noise. This is because the signal arising from moving spots contributes significantly less intensity to a certain pixel of the average image while a stationary object contributes similar intensity to a pixel in each frame over the same acquisition time. Brightness contrast for all maximum projection images presented here was slightly adjusted for clarity in visualization of SM dynamic behaviors.

2.5. Single-Molecule Tracking (SMT) and Data Analysis. Following preliminary processing of the acquired movies, we chose different regions of interest (ROIs) to ensure that spatially well-separated SMs were being monitored. In order to distinguish SMs from background noise, only those emission spots were analyzed which had SBR greater than ~4, and full width at half-maxima (fwhm) of less than 250 nm. To locate the spatial positions of individual molecules over time, each cropped movie containing data of a SM was analyzed using a SMT program written in Matlab 7. To obtain sub-diffraction-limited spatial resolution, the center of the point spread function (PSF) was located by fitting the data in each frame (within the ROI) using a 2D Gaussian function[52]

$$I(x, y) = A_0 \exp(-[(x - x_0)^2 + (y - y_0)^2]/2\sigma^2) \quad (1)$$

where A_0 is the amplitude at the maxima position (x_0, y_0) of the fitted peaks and σ is related to the fwhm. The accuracy of locating the positions of SMs using this method was found to be slightly better than that calculated using centroids of the diffraction-limited emission spots, but both methods yielded qualitatively similar results at high RH. In our experiments, for a typical SBR of ~5, the spatial resolution calculated from the standard deviation of the data is found to be less than 25 nm. Therefore, as a conservative estimate, individual tracers which undergo position fluctuations within 33 nm were considered to be immobile; i.e., the static localization error[53,54] was <0.001 μm^2.

Using the coordinates of SMs obtained for each trajectory ($\{\vec{r}(t_i)\} = \{x(t_i), y(t_i); i = 1,2,...\}$), the mean square displacements (MSDs) were calculated for lag times (τ) up to 20% of the total number of acquired frames (N) using[55,56]

$$\langle r^2(\tau)\rangle = \langle[\vec{r}(t_i + \tau) - \vec{r}(t_i)]^2\rangle \quad (2)$$

where $\vec{r}(t_i)$ and $\vec{r}(t_i + \tau)$ are positions of the molecule at time t_i and $t_i + \tau$, respectively, and t_i runs till $t_N - \tau$. For a random walker (molecule) undergoing Brownian diffusion, the micro-diffusion coefficient (D_μ) can be obtained from the MSD against τ plots using[57,58]

$$\langle r^2\rangle = 2nD_\mu\tau \quad (3)$$

where n denotes the dimensionality. In reality, even though individual tracers traverse along all three spatial directions (i.e., along x, y, and z in laboratory frame) in a thin film, quantitative information on movement along vertical (z) direction could not be obtained reliably due to the low z-resolution of our microscope. This is because fluorescence intensity variations associated with z-movement of SMs in a ~200 nm thick film is far less than those due to changes in absorption cross sections arising from molecular reorientation.[25] Therefore, we essentially probe the 2D projection of the 3D motion of Rh6G molecules; i.e., we consider translational motion dominates along lateral directions of the thin film. Under this assumption, D_μ is obtained from best fit of the initial slopes of MSD versus τ

$$\langle r^2\rangle = 4D_\mu\tau \quad (4)$$

We chose a minimum τ of up to 1 s to estimate D_μ using eq 4 even for those MSD curves which deviate from linearity over larger elapsed time because fitting the data with less than 10 points leads to larger uncertainty in determination of D_μ.[59] For some molecules, MSD curves show nonzero intercept (ε), which were fit to the expression $\langle r^2\rangle = 4D_\mu\tau + \varepsilon$.[53,60] However, for most such tracers, the values of D_μ obtained using this expression did not vary significantly from those obtained using eq 4.

Since SMs often displayed fluorescence intermittency (blinking), we selected those molecules with lowest frequency of excursions to the "off" state during its lifetime, and the frames for which the molecules blinked were not included for MSD analyses. Further, all the SMs photobleach after a certain time depending on the molecule and ambient RH. Molecules which survived for less than 5 s (50 frames) were not chosen for generating MSD curves due to lack of statistical relevance and uncertainty associated with determination of D_μ (with very few lag-times).[61] However, these short trajectories were included in generating displacement−jump distributions,

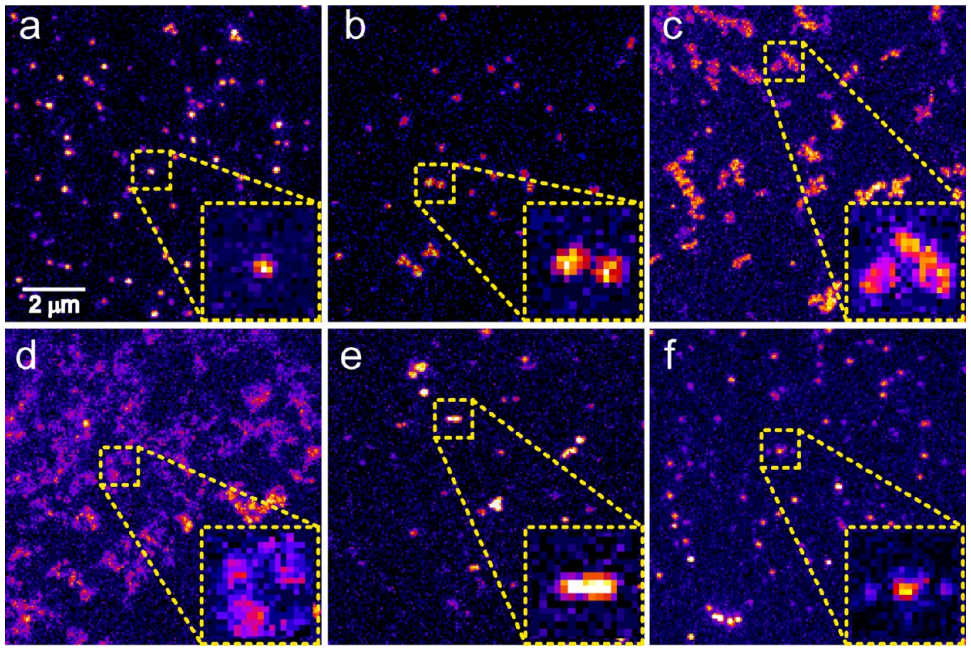

Figure 3. Maximum projection fluorescence intensity images (for 10 s) of Rh6G in PVP thin films collected after 30 min of exposure at a given RH, with insets showing a blowup of 1 × 1 μm^2 area. Images obtained for ~200 nm film at (a) RH ≤ 20% (argon environment), (b) RH ~ 60%, and (c) RH ~ 75%. Images obtained for tracers (d) near polymer−air interface at RH ~65%, (e) within a ~500 nm thick film at RH ~75%, and (f) after removal of ambient moisture (by purging argon for ~20 min) for a ~200 nm film, showing arrest of molecular motion. The scale bar is the same for all the images. Movies (up to 5 s) using which (a−d) were constructed are provided in the Supporting Information as movies 001−004.

$P(\Delta q)$, where $\Delta q = \Delta x$ or Δy for $\tau = 0.1$s, which were plotted at 50 nm bins. Local microviscosities (η_μ) experienced by individual tracer molecules were calculated using the Stokes−Einstein relation, $D_\mu = k_B T/6\pi\eta_\mu a$, where $k_B T$ is the thermal energy and a is the radius of Rh6G. It is noted that each SM reports an average D_μ (and hence an average local viscosity) for the given spatial region of the matrix where that particular tracer navigates.

For tracers undergoing non-Brownian motion, the slopes of the MSD plots deviate from linearity and such anomalous subdiffusion is described by power-law scaling[62]

$$\langle r^2 \rangle \propto \tau^\alpha \tag{5}$$

where α is the power-law exponent and subdiffusion is characterized by $0 < \alpha < 1$. While values for α are not reported due to the limited number of points (lag times) used to fit the experimental MSD curves using eq 5, subdiffusive motion was identified from the slope of MSD curves plotted in log−log scale. When a tracer undergoes confined (corralled) motion, the MSD curves shows saturation behaviors, which can be fitted to the expression.[62]

$$\langle r^2 \rangle \approx r_c^2[1 - A_1 \exp(-4A_2 D_\mu \tau / r_c^2)] \tag{6}$$

where r_c^2 is the corral size and A_1 and A_2 are constants which depend on confinement geometry. Estimates of r_c^2 were obtained from the saturation values of experimental MSD plots.

The normalized velocity autocorrelation function, $C_v(\tau) = \langle \vec{v}(t)\cdot\vec{v}(t+\tau)\rangle / \langle v^2(t)\rangle$, was calculated from the velocity data which were extracted from each SM trajectory $\{\vec{r}(t_i)\}$. The velocity $\vec{v}(t) = [\vec{r}(r+\delta) - \vec{r}(t)]/\delta$ is computed from the difference in position of the molecule between two successive frames, δ being the minimum time interval of 0.1 s. Thus, for each particle trajectory, we evaluate the velocity time series $\{\vec{v}(t_i)\} = \{v_x(t_i), v_y(t_i);\ i = 1,2,...\}$ and then compute $C_v(\tau)$.

3. RESULTS AND DISCUSSION

3.1. Mobility of Tracers in PVP Thin Films under Different Ambient RH. Due to lack of a priori knowledge on the extent of T_g lowering for PVP thin films at a specific ambient RH, we have investigated the dynamics of Rh6G in PVP films with increasing levels of ambient moisture. Figure 3a−c shows the maximum projection images of Rh6G probes sparsely distributed in PVP thin films at three different humidity regimes (see movies 001−003 in Supporting Information). Under dry conditions (ambient RH <20%), well-separated diffraction-limited fluorescent spots are visible (Figure 3a) which suggests that probe molecules remain stationary. With increasing RH of up to ~50%, no apparent spatiotemporal changes in the PSFs could be noticed. However, upon slight increase in the ambient humidity to ~55%, several non-diffraction-limited fluorescent spots (with fwhm of ~300−500 nm) are readily observed, which indicates that Rh6G molecules become translationally active above a certain range of critical RH (50−55%). Further, at RH of ~60%, a considerable proportion of Rh6G molecules are found to exhibit enhanced translational mobility (Figure 3b), while at even higher RH of 75%, individual tracers display distinct and extended tracks (Figure 3c), suggesting that diffusion dynamics is augmented significantly.

To eliminate the possibility that the observed diffusion dynamics does not arise from tracer molecules located near the polymer−air interface, we have visualized the dynamic behaviors of Rh6G spin-cast on top of a preformed PVP thin film. We find that a vast majority of tracers display remarkably fast movement (see movie 004, Supporting Information) even at moderate RH levels, resulting in obscure images (Figure 3d) where individual tracks cannot be distinguished. Such contrasting behaviors (Figure 3, b, c, and d) suggest that the tracer dynamics observed in Figure 3b,c is due to Rh6G buried

dx.doi.org/10.1021/jp401704e | J. Phys. Chem. B 2013, 117, 7771−7782

within the polymer network. Therefore, we attribute the changes in SM translational mobility with increasing ambient RH (Figure 3a–c) to moisture absorption induced softening of the PVP matrix (i.e., plasticization). Penetration of water molecules within the polymer network leads to a decrease in inter-/intrachain interactions (i.e., increase in free volume), and swelling of the network (Figure 1) allows the tracers to undergo translational motion. Since the extent of moisture penetration into the polymer matrix (over 30 min) is expected to depend on film thickness, experiments were performed on thicker (~500 nm) PVP films where tracers are buried deep into the PVP matrix. We find that, under these conditions, Rh6G typically takes several hours to display translational motion even at a high RH of ~75% (Figure 3e), consistent with our hypothesis.

Interestingly, the swelling/softening of the PVP film due to uptake of ambient moisture (i.e., the process of plasticization) is found to be reversible to a certain extent. Upon removal of moisture within the enclosed chamber (by purging argon gas for ~20 min), the translational dynamics of a vast majority of probe molecules is found to be arrested considerably (Figure 3f) as compared to that at high RH levels (Figure 3c). While it is known that complete removal of (residual) solvents in polymer films is extremely difficult,[36] here it is likely that sufficient amount of water molecules are removed from the PVP matrix to arrest translational mobility of Rh6G. This indicates that quasi-equilibrium (for moisture uptake at fixed RH levels) is attained within a relatively short time for ~200 nm thin films. Therefore, it was possible to probe the PVP thin film samples under different moisture contents by fixing the ambient RH to a certain level before each measurement. This allowed us to visualize the variations in dynamics behavior of individual tracers and thereby obtain information on the local rigidity or viscosity of PVP thin films at different moisture contents.

In the following sections, we describe how dynamics of individual Rh6G tracers is affected upon varying ambient humidity on PVP thin films, which reflect the physical changes in the network with increasing moisture content.

3.2. PVP Thin Film under Ambient RH of up to 50%.

As mentioned earlier, under low ambient RH (20–50%), no spatiotemporal fluctuations of emission spots could be detected till the molecules photobleach irreversibly. Figure 4a,b shows a typical track and temporal evolution of the positions for a Rh6G molecule under dry conditions of the film (RH < 20%). The standard deviation of displacements in such traces is found to be less than 25 nm, and MSD plots (Figure 4b, inset) have a slope of less than 5×10^{-4} μm^2 s^{-1}. However, from Figure 4a,b, it is difficult to establish whether the Rh6G molecule is truly stationary or undergoes localized translational motion within few tens of nanometers.[12] This necessitates the investigation of rotational rigidity of individual probes, as translationally active Rh6G molecules are expected to be rotationally mobile.[26]

Figure 4c shows a maximum projection image of Rh6G molecules in the dry PVP matrix obtained under TIRF illumination, which has been previously utilized to obtain information on the rigidity of vertically oriented SMs.[46] Here, in addition to other near-Gaussian diffraction-limited spots, several doughnut-shaped emission patterns are observed, characteristic of rigid molecular transition dipoles oriented out of plane (i.e., along z-direction).[46] Figure 4d shows the transient nature of such SM emission patterns, which indicates that vertically aligned Rh6G molecule can undergo wobbling

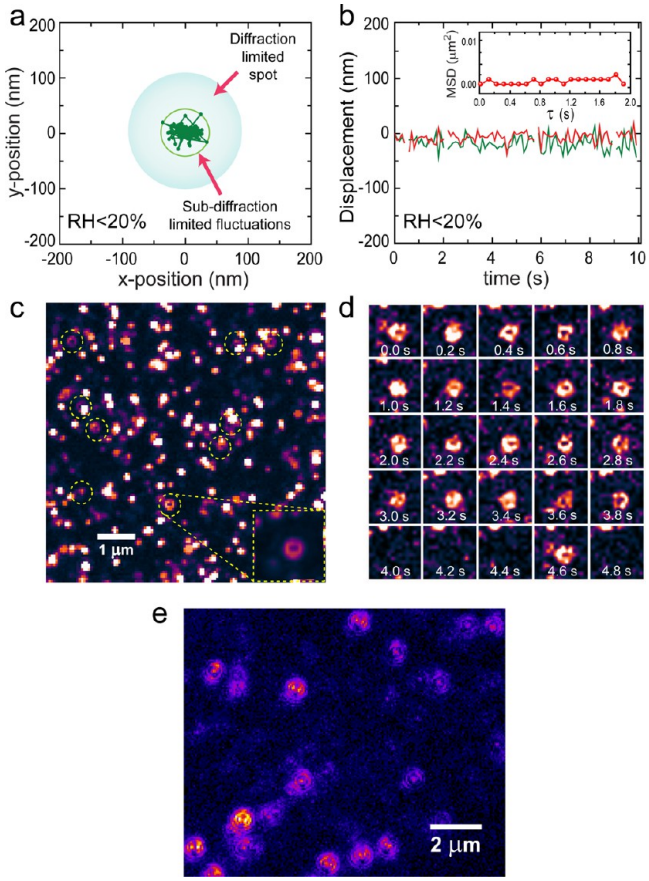

Figure 4. (a) 2D x–y tracks of a Rh6G molecule in PVP in argon environment. (b) Time trajectories of x (red) and y (green) positions, the same tracer molecule showing sub-diffraction-limited spatial resolution. The MSD vs τ plot for this stationary molecule is shown as inset. (c) Maximum projection images (5 s) of a larger area of the PVP film at RH 20%. Non-Gaussian-shaped emission patterns are marked with dotted circles and one of them is blown up as inset. (d) Temporal evolution of a characteristic doughnut emission pattern. This molecule shows wobbling motion between 0 and 3.8 s, "blinks" between 4 and 4.4 s, and eventually photobleach after 4.6 s. (e) Defocused image (5 s average) of Rh6G in PVP film at RH ~ 50%, which shows the presence of both rotationally immobile molecules (highly asymmetric dumbbell patterns) and molecules which reorient at time scales faster than 1 Hz (more symmetric patterns with bright central spot).

motion within the polymer cavity. This strongly suggests that, under dry conditions, the probe molecules are entrapped in a highly rigid local environment (or compact voids). However, upon increase in the moisture content of the matrix (at RH ~ 40%), the occurrence of such non-Gaussian emission patterns is found to be less frequent. Moreover, near the critical RH (~50%) almost all the emission spots display near-Gaussian PSF, from which it is difficult to comment on their rotational mobility. To clarify this ambiguity and obtain qualitative information on rotational activity, we performed defocused imaging measurements[10] at RH of 50% (Figure 4e), and compared these SM emission patterns with reported simulations.[16,48] The asymmetric intensity distributions observed in Figure 4e reveals that a nonnegligible proportion of SMs undergo reorientation over seconds time scales, which supports our earlier inference the tracers are translationally inactive even at RH of 50%.

dx.doi.org/10.1021/jp401704e | J. Phys. Chem. B 2013, 117, 7771–7782

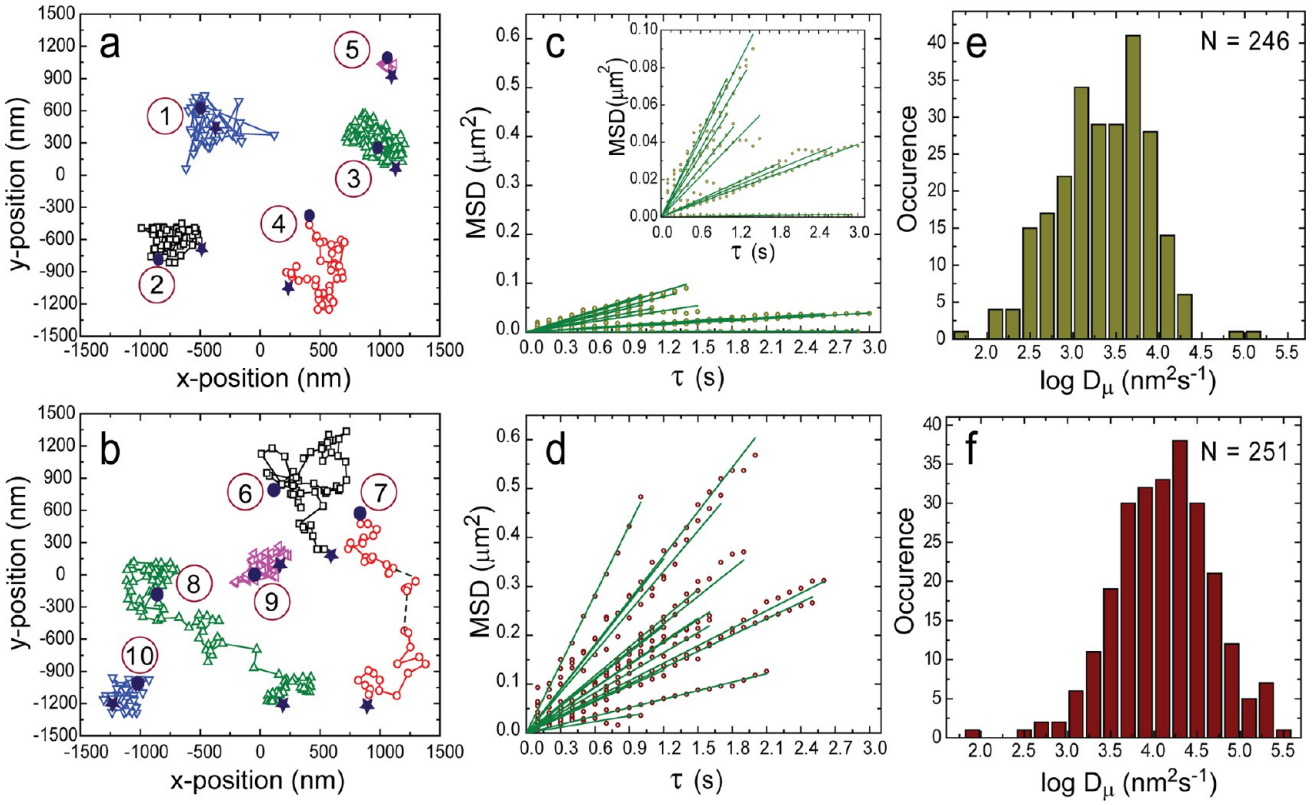

Figure 5. 2D (x–y) tracks of individual Rh6G molecules at (a) RH 60% and (b) RH 75% collected over a minimum period of 5 s. The filled circles and the stars represent the beginning and the end of the trajectories. MSD plots for representative molecules at RH 60% (c) and RH 75% (d) which show linear progression with elapsed time (τ). Inset in (c) shows the same MSD plots blown up for clarity. In (c) and (d), the experimental data (symbols) were fitted (line) using eq 4. Distribution of D_μ (in logarithmic scale) for ~250 tracers obtained at RH 60% (e) and RH 75% (f).

In addition to confirmation of probes being stationary near the threshold RH, an interesting aspect regarding plasticization emerges from SM rotational diffusion experiments. It is clear that a larger proportion of Rh6G molecules undergo faster reorientation in RH range of 40–50% as compared to that in dry conditions, which suggests that the PVP network swells slightly even under relatively low amount of absorbed moisture. We note that the initiation of rotational diffusion for SMs in other polymer thin films (such as poly(methyl acrylate) (PMA) and poly(styrene) (PS)) has been shown to be a qualitative measure of the T_g since molecular reorientation is amplified significantly when the T_g is close to (or slightly below) measurement temperatures.[21,63] It is therefore reasonable to conclude that with increase of ambient RH from 20% to 40%, the onset of plasticization results in a rather dramatic lowering of the effective T_g of the PVP thin film (from >400 K to the range of 300–320 K). This is quite surprising, given that plasticization of bulk PVP of similar molecular weight requires considerably more moisture for lowering its T_g close to room temperature.[43,44] SM rotational diffusion measurements are currently underway to investigate the physical properties of PVP matrix at low moisture contents.

3.3. PVP Thin Film under Ambient RH of 55–75%. As mentioned in section 3.1, translational mobility of Rh6G molecules is found to be initiated only at a threshold humidity level of ~55% for PVP thin films of ~200 nm thickness. Temperature-dependent tracer diffusion dynamics reported for other polymer thin films (such as PS and PMA) have shown that unambiguous translational movement (beyond ~50 nm) of SMs probes could be detected when measurements were performed at ~1.1T_g of the polymer.[11,21,24] Therefore, it is likely that beyond RH of 55%, the amount of moisture absorbed within the polymer thin film is high enough to reduce the effective T_g close to or below 273 K. Above an ambient RH of ~60%, a majority (~70%) of the fluorescent tracers displayed considerable lateral movement (Figure 3b), and many of these molecules could be tracked reliably. Figure 5a,b shows representative SM trajectories of the translational motion exhibited by Rh6G at two higher humidity levels (60% and 75%), where a wide variety of tracer mobility could be observed. For freely diffusing molecules undergoing 2D random walk (i.e., Brownian motion in a thin film), information on their diffusivities can be extracted from the slope of MSD plots, which is expected to increase linearly with elapsed time (τ).[57,62] However, we find that only a fraction of Rh6G tracers exhibits linear progression of MSD with τ, several of which are shown in Figure 5c,d for ambient RH of 60% and 75%. It is apparent that the slopes of the MSD curves have (i) quite a large spread at both the RH levels, which indicates inhomogeneity of the polymer matrix, and (ii) are steeper for a larger proportion of tracers at higher ambient RH, suggesting an increase in the diffusivity of Rh6G with increasing moisture content of the PVP thin film.

The diverse range of slopes observed in the MSD plots (Figure 5c,d) necessitates the analyses of a large number of SM trajectories at each RH level, in order to estimate the range of microscopic diffusion coefficient, D_μ. Figure 5e,f shows the distribution of D_μ, obtained from the initial slope of each MSD curve, for several hundred SM trajectories under ambient RH of ~60% and ~75%. The distributions of D_μ span almost 3 orders

dx.doi.org/10.1021/jp401704e | J. Phys. Chem. B 2013, 117, 7771–7782

of magnitude (the range of D_μ^{RH60} is $\sim(0.13-20) \times 10^{-3}$ μm^2 s^{-1}, while that for D_μ^{RH75} is $\sim(0.5-300) \times 10^{-3}$ μm^2 s^{-1}), with considerable overlap in D_μ values. The average value of D_μ is found to increase by a factor of 6 (from $\sim 4.78 \times 10^{-3}$ to $\sim 27.78 \times 10^{-3}$ μm^2 s^{-1}) upon increase of ambient RH from 60 to 75%, which is a consequence of the population distribution of molecules with different values of D_μ. This indicates that the proportion of tracer molecules which experience lower effective viscosities (or microviscosities, η_μ), considered as a semi-quantitative measure of plasticization, becomes larger with increasing moisture absorption of the PVP thin film. We estimate using Stokes–Einstein relation that η_μ is reduced from $\sim$1000 to $\sim$1 N sm^{-2} upon increase in moisture content of the film (from RH of 60 to 75%). It is noted however, that these values of η_μ do not reflect the decrease in average viscosity of the entire polymer matrix, as Figure 5e,f points out that η_μ fluctuates considerably even at a fixed RH level. Rather, they provide a qualitative upper and lower bound of the effective viscosity in local microscopic domains of the PVP thin films undergoing plasticization.

Here, we should mention that MSD curves (Figure 5c,d) were constructed from those SM tracks which lasted for >5 s because of the uncertainty in estimation of D_μ for tracers which photobleach within a few seconds. However, these short trajectories could be utilized along with SMs which survive longer durations to generate statistically well-averaged displacement–jump distributions, $P(\Delta q)$, where $\Delta q = \Delta x$ or Δy for τ = 0.1 s. This aspect is clearly manifested in the semilogarithmic plot of $P(\Delta q)$ (Figure 6), which is quite smooth as compared

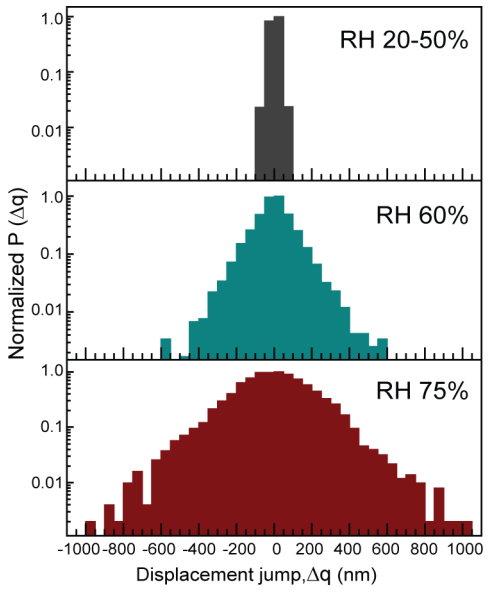

Figure 6. Displacement–jump distributions, $P(\Delta q)$, for τ = 0.1 s, at three regimes of ambient moisture: 20–50% (top panel), ~60% (middle panel), and ~75% (bottom panel). These were generated from 100 trajectories at each RH, with 50 nm binning.

to the relatively noisy MSD curves. The broadening of the distribution with increase in moisture absorption of the PVP matrix validates the increasing trend of D_μ estimated from MSD curves, and reflects the decreasing resistance offered by the medium. Further, we note that MSD is influenced by the standard deviation (σ) of the displacement jumps, $P(\Delta q)$ as well as the temporal correlations in the jumps,[64] but not so much by the detailed nature of $P(\Delta q)$ itself.[65] For example, in a true Markovian process where the successive jumps are uncorrelated, $D = \sigma^2/(4\delta t)$, where δt is the time interval between successive jumps.[66] This follows from the central limit theorem irrespective of whether $P(\Delta q)$ is Gaussian, exponential, or some other distribution. On the other hand, $P(\Delta q)$ reveals information about the microscopic process,[67] and it was therefore important to check the nature of the distribution. Intriguingly, contrary to the expected Gaussian behavior, we find $P(\Delta q)$ to be close to exponential, especially for the partially plasticized network at intermediate RH (Figure 6b). Interestingly, it has been shown that despite $P(\Delta q)$ being exponential at small elapsed times, the MSD is still linear in τ, which is attributed to "*slowly varying, heterogeneous fluctuations of the environment*" where tracers navigate.[67]

3.4. Heterogeneity during Plasticization of PVP. The observed dynamic behavior of SM probes is a consequence of polymer morphology in the vicinity of individual tracers and how the local network structure as well as relaxation processes therein is affected in the presence of percolating water molecules. Interestingly, even under RH levels of 60 and 75%, some Rh6G probes always appear to be static, and the fraction of such immobile tracers decrease with increasing moisture content of the PVP thin film (Table 1). This behavior

Table 1. Fraction of Rh6G Molecules Which Undergo Various Types of Translational Motion

	category of motion			
RH (%)	immobile	confined motion	subdiffusion	normal diffusion
20–50	0.96	0.04	–	–
~55	0.64	0.31	0.04	0.01
60 ± 2	0.23	0.06	0.47	0.24
75 ± 2	0.08	0.04	0.57	0.31

is likely due to location of some tracers at specific rigid domains within the matrix (such as highly entangled polymer chains or regions of high polymer density) which might not be severely affected by absorbed moisture. The immobility of a certain fraction of SMs, as well as the wide span of diffusivities for mobile tracers (Figure 5), reflects the spatial inhomogeneity of the (partially) plasticized PVP thin-film network. One possibility is that diverse spatiotemporal behaviors of SMs arise from the location of tracers at different depths (along the z-direction) in the thin film. For instance, Rh6G molecules located farther from the glass–polymer interface can experience far lower effective viscosity, and therefore have higher mobility as compared to those buried deeper into the matrix (Figure 3f). The proposition that moisture absorption induced softening of PVP films is depth dependent is consistent with a recent report where it has been shown that the effective T_g of amorphous polymer thin films is a function of distance from the polymer–air interface.[23] It should be noted, however, that the variation of local viscosities due to differential extent of moisture absorption along lateral dimensions of the thin film cannot be ruled out.

Further insight on heterogeneity of the PVP matrix undergoing plasticization could be obtained by categorizing the nature of translational motion on the basis of MSD curves, at RH regime of 55–75% (Figure 7a–c). We find that, in this entire RH range, only a limited proportion of Rh6G molecules show a linear progression of MSD (Figure 7c) as expected of normal (Brownian) diffusion. On the contrary, a considerable fraction of MSD curves exhibit anomalous (non-Brownian)

dx.doi.org/10.1021/jp401704e | J. Phys. Chem. B 2013, 117, 7771–7782

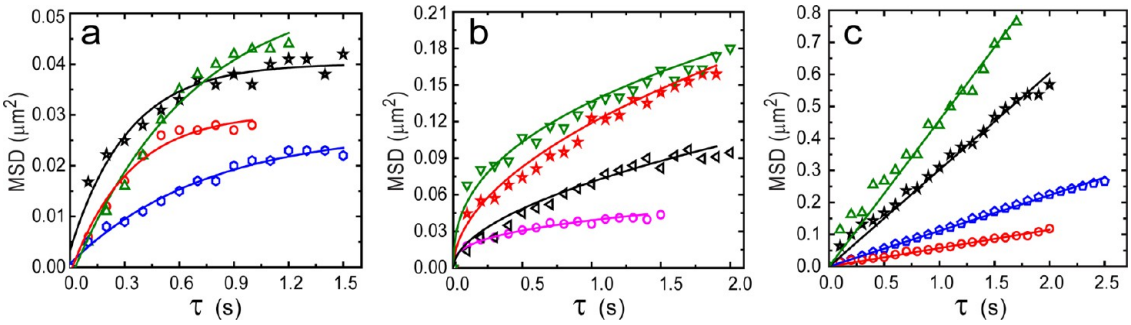

Figure 7. Representative MSD vs τ plots exhibiting (a) confined, (b) anomalous, and (c) Brownian behavior for four individual Rh6G molecules obtained under RH regimes (>55%) which allow for translational mobility. The symbols represent experimental data, and the lines are the best fit to expressions for confined motion, subdiffusion and normal diffusion (see section 2.5).

behaviors, specifically subdiffusion (Figure 7b) and confined (corralled) diffusion (Figure 7a), summarized in Table 1. While a majority of Rh6G molecules at RH of ∼55% are static, those which are translationally active undergo confined motion (within 0.01−0.1 μm^2), suggesting preferential softening of certain nanoscale regions of the thin-film matrix. At slightly higher moisture content of the film, mobile tracer exhibits predominantly subdiffusion or normal (Brownian) diffusion; we envisage that, at RH of ∼60%, partially plasticized "softer" zones spread across larger lateral dimensions (∼few μm^2). With further increase in absorbed moisture, these domains of lower (but not necessarily uniform) viscosity become large enough to coalesce together, which ultimately propagates into plasticization of the entire PVP film. Therefore, the initiation of translational motion of tracers at localized regions, which is at first confined and eventually extends to either Brownian motion or anomalous subdiffusion (depending on the SM), points out to the gradual but nonuniform changes in the physical properties of the PVP thin-film matrix with increasing moisture content.

The coexistence of different types of translational diffusion at various RH reinforces the high degree inhomogeneity during the process of softening/swelling of PVP matrix, and is somewhat reminiscent of SM tracer dynamics in polymer films near or above T_g.[21,23,24] Static heterogeneity, as discussed earlier, is relatively simple to understand; different spatial locations of polymer matrix have significant variation in viscosities (or the local T_g) even at fixed atmospheric moisture content. However, information on dynamic heterogeneity is difficult to extract from SM diffusion dynamics because each tracer encounters different spatial locations during the course of its movement. Nonetheless, it is possible that diversity in translational motion is due to a different response to moisture absorption at various regions in the network. For instance, extent of swelling of polymer films is known to severely affect molecular diffusivity, which has been related to stress fields induced by morphological changes in the polymer matrix arising from solvent penetrants.[68] While the thin films studied here have been annealed for several hours to allow for relaxation, local regions of PVP network can have differential stress induced by percolating water molecules. Alternatively, since plasticization of the PVP film results in lowering of the T_g even below ∼295 K (where primary relaxation processes become dominant), morphology of the polymer matrix can undergo dynamic changes at time scales comparable to the motion of tracer molecules,[10,21] which can also lead to their diverse dynamic behaviors.

3.5. Origin for Subdiffusive Behavior of Mobile Tracers. While it is relatively simple to interpret confined motion or normal diffusion, actual mechanisms that lead to subdiffusive behaviors can be hard to interpret even in terms of the power law exponent (α).[64,69] It is noted that the subdiffusive behavior of mobile tracers in hydrated films is not very surprising considering the extremely crowded environment of the polymer matrix.[64,69,70] For instance, subdiffusion has been reported for molecular tracers within live cells, which have been attributed to macromolecular crowding of the local microenvironment.[69−71] Hindered motion through a dense viscous media in the presence of high concentration of obstacles,[72] or even a combination of corralled and Brownian motion, can result in subdiffusive behaviors.[71,72] To distinguish among the various possibilities that lead to subdiffusion of tracer molecules in the plasticized PVP matrix, we computed the normalized, nonequal time velocity−velocity correlation function from individual tracer trajectories: $C_v(\tau) = \langle \vec{v}(t)\cdot\vec{v}(t+\tau)\rangle/\langle v^2(t)\rangle$. Figure 8a,b shows the MSD vs lag time (τ) and the velocity correlation functions ($C_v(\tau)$) for 108 trajectories obtained at RH of 75%. The slope of the MSD plots (Figure 8a) in log−log scale reveals that majority of these tracer molecules show subdiffusive behaviors. Interestingly, the velocity autocorrelation functions (Figure 8b) demonstrate that most of these trajectories exhibit a *negative* correlation at very short τ evident from the average of all the 108 correlation functions (bold line).

Such negative correlations at initial times can arise from two different mechanisms, namely fractional Brownian motion (FBM) and continuous time random walk (CTRW) in the presence of confinement.[60,64] FBM is typically associated with the motion of a Brownian walker in a viscoelastic medium. A polymer network is known to have strong viscoelastic properties;[70] the elasticity arises from the entropic elasticity of the entangled polymers, and the viscosity (or equivalently friction) originates from the hindrances provided by the polymer meshwork. One prominent example of a viscoelastic medium is the cytoplasm of a cell, where the presence of various macromolecules and cytoskeletal filaments in the cell cytoplasm renders viscoelastic properties to the cytoplasm, leading to FBM.[71] In such a medium, when a random walker takes a step in some direction, due to the elastic effect it is partially pulled back toward the origin; i.e., it retains some memory. This implies that the velocities of the walker at successive time instants are opposite to each other, which leads to negative (or anti) correlation in the velocity of the tracers at short lag times (τ). To check whether the subdiffusion of tracer

dx.doi.org/10.1021/jp401704e | J. Phys. Chem. B 2013, 117, 7771−7782

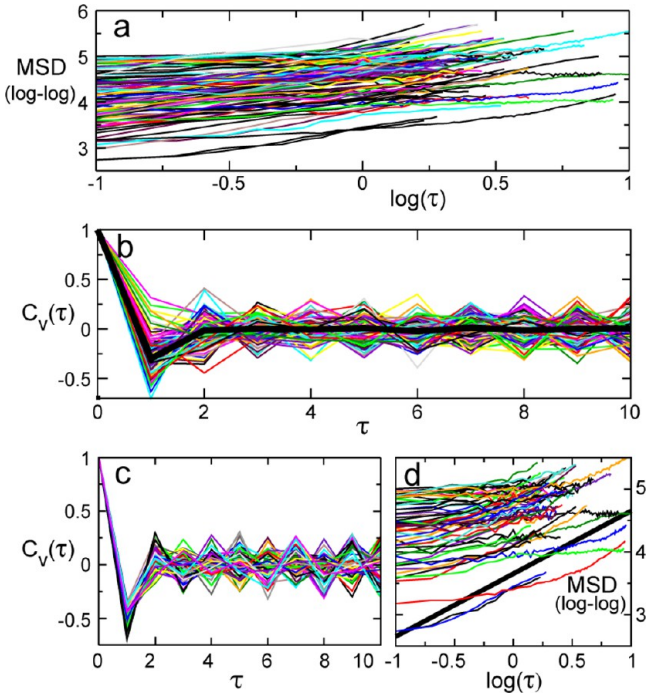

Figure 8. Characteristics of the tracer diffusion obtained under RH of 75%. The log−log plot (a) of the MSD vs τ for 108 SM trajectories. The normalized velocity autocorrelation function $[C_v(\tau)]$ (b) plotted as a function of τ. Velocity correlation functions of 57 trajectories (c) which exhibit significant anticorrelation, and their corresponding MSD plots (d). The thick solid line in (d) displays the MSD for a simple Brownian walker. For all plots, τ is represented in frames.

molecules are indeed due to FBM, we selected 57 of the 108 trajectories (Figure 8c) which showed a prominent negative correlation (with maximum negativity less than −0.3) and found that a vast majority of these exhibit subdiffusive behaviors (Figure 8d). On the contrary, the trajectories with nonnegative velocity correlation were found to predominantly undergo normal Brownian diffusion.

The alternative mechanism for subdiffusion of tracers is confined CTRW. Typically, CTRW arises from a situation where the random walker intermittently pauses for an interval and then moves, leading to broad waiting time distributions.[64,71] However, this characteristic is absent in our situation; rarely do we observe SM trajectories which display significant pauses or large jump lengths (at RH of 60−75%), which suggests that CTRW might not be operational during tracer navigation through the plasticized PVP matrix. Furthermore, it has been shown that, within the CTRW model, negative correlation arises only in the presence of confinement,[64] i.e., localized movement in a microenvironment where the tracer resides. However, most of the MSD plots in Figure 8a do not show saturation effects, ruling out confined CTRW as a possible source of negative correlation observed for majority of trajectories (Figure 8b). This leads us to conclude that the subdiffusive motion of tracer molecules navigating through plasticized PVP matrix arises due to fractional Brownian motion.

4. CONCLUSIONS

We have probed the diffusion dynamics of individual Rh6G molecules to investigate the effect of ambient moisture absorption on PVP thin films. It is found that increasing moisture content of the polymer film induces significant morphological changes in the polymer matrix, which affects both rotational and translational diffusion of single-molecule tracers. Upon exposure to low amounts of water vapor (RH of ∼30%), the polymer network swells slightly to allow for rotational mobility of the probes residing therein, indicating onset of plasticization. However, we find that, only beyond a threshold RH of ∼55%, the rigidity of the matrix is low enough to allow for translational diffusion of tracers to occur. Even at this RH, only ∼30% of the tracers are mobile and display primarily confined motion, suggesting selective softening of nanoscale regions within the polymer film. With slight increase in the moisture content (at RH of 60%), a vast majority of tracers become translationally active and undergo diverse dynamic behaviors. Our results suggest that, with gradual increase in the ambient RH, these domains of lower viscosity progressively increase in size and eventually coalesce, leading to plasticization of the entire matrix. We find that changing the ambient RH from 60 to 75% results in ∼6-fold increase in average values of microdiffusion coefficient (D_μ) for tracers. However, the distributions of D_μ at these two RH levels span several orders of magnitude, indicating the extremely inhomogeneous viscous nature of the plasticized PVP matrix. The heterogeneity of the PVP film in the presence of absorbed moisture is further reiterated by the presence of some stationary molecules and the coexistence of anomalous and normal (Brownian) tracer diffusion at relatively high RH of 60−75%. Intriguingly, we find that, over this entire RH regime, the majority of the Rh6G molecules undergo subdiffusive motion. To investigate the origin of subdiffusive behavior exhibited by the tracers, single-molecule trajectories were analyzed to compute the velocity autocorrelation function, which shows a prominent negative peak at short lag times. We argue that the mechanism of subdiffusion of tracer molecules in the plasticized PVP matrix is most likely fractional Brownian motion, similar to the diffusion dynamics exhibited by tracers in viscoelastic media such as the cellular cytoplasm. Therefore, the findings of this study using PVP as a model system can be useful to further understand diffusion of entrapped molecules in polymer thin films under hydrating conditions.

■ ASSOCIATED CONTENT

Supporting Information

Supplementary movies of single-molecule diffusion behaviors at various ambient RH are provided as movies 001−004. This material is available free of charge via the Internet at http://pubs.acs.org.

■ AUTHOR INFORMATION

Corresponding Author

*E-mail: arindam@chem.iitb.ac.in. Tel.: (+91)2225767154.

Present Addresses

[¶]Department of Chemistry, Carnegie Mellon University, Pittsburgh, PA 15213.

[⊥]Max-Planck Institute for the Physics of Complex Systems, 01187 Dresden, Germany.

Notes

The authors declare no competing financial interest.

■ ACKNOWLEDGMENTS

S.B., D.K.S., and S.D. thank CSIR (India) for Ph.D. scholarships and grant (Scheme 80(0070)/08/EMR-II)

awarded to A.C. for partial support of this work. We acknowledge IRCC, IIT Bombay, for partial funding, and the Departments of Physics and Chemical Engineering for usage of central facility instruments. We thank Drs. R. Chakrabarti, R. M. Thaokar, and P. Sunthar for valuable discussions and critical comments, and Dr. G. N. Patwari for providing us with rhodamine 6G.

REFERENCES

(1) van Zanten, J. H.; Wallace, W. E.; Wu, W.-I. Effect of Strongly Favorable Substrate Interactions on the Thermal Properties of Ultrathin Polymer Films. *Phys. Rev. E* **1996**, *53* (3), R2053−R2056.
(2) Luengo, G.; Schmitt, F. J.; Hill, R.; Israelachvili, J. Thin Film Rheology and Tribology of Confined Polymer Melts: Contrasts with Bulk Properties. *Macromolecules* **1997**, *30*, 2482−2494.
(3) Alcoutlabi, M.; McKenna, G. B. Effects of Confinement on Material Behavior at the Nanometre Size Scale. *J. Phys.: Condens. Matter* **2005**, *17* (15), R461−R524.
(4) Fukao, K.; Miyamoto, Y. Glass Transitions and Dynamics in Thin Polymer Films: Dielectric Relaxation of Thin Films of Polystyrene. *Phys. Rev. E* **2000**, *61* (2), 1743−1754.
(5) Ediger, M. D. Spatially Heterogeneous Dynamics in Supercooled Liquids. *Annu. Rev. Phys. Chem.* **2000**, *51* (1), 99−128.
(6) Hilles, H. M.; Ortega, F.; Rubio, R. G.; Monroy, F. Long-Time Relaxation Dynamics of Langmuir Films of a Glass-Forming Polymer: Evidence of Glasslike Dynamics in Two Dimensions. *Phys. Rev. Lett.* **2004**, *92* (25), 255503.
(7) Torres, J. M.; Stafford, C. M.; Vogt, B. D. Elastic Modulus of Amorphous Polymer Thin Films: Relationship to the Glass Transition Temperature. *ACS Nano* **2009**, *3*, 2677−2685.
(8) Ahn, S. Il.; Yoon,s, J. G.; Kim, J. H.; Zin, W. C. Effect of Water Contact on the Density Distributions of Thin Supported Polymer Films Investigated by an X-ray Reflectivity Method. *Langmuir* **2010**, *26*, 18483−18490.
(9) Moerner, W. E. A Dozen Years of Single-Molecule Spectroscopy in Physics, Chemistry, and Biophysics. *J. Phys. Chem. B* **2002**, *106*, 910−927.
(10) Wöll, D.; Braeken, E.; Deres, A.; De Schryver, F. C.; Uji-I, H.; Hofkens, J. Polymers and Single Molecule Fluorescence Spectroscopy: What Can We Learn? *Chem. Soc. Rev.* **2009**, *38* (2), 313−328.
(11) Kaufman, L. J. Heterogeneity in Single-Molecule Observables in the Study of Supercooled Liquids. *Annu. Rev. Phys. Chem.* **2013**, *64*, 177−200.
(12) Bopp, M. A.; Meixner, A. J.; Tarrach, G.; Zschokke-Gränacher, I.; Novotny, L. Direct Imaging Single Molecule Diffusion in a Solid Polymer Host. *Chem. Phys. Lett.* **1996**, *263* (6), 721−726.
(13) Bartko, A. P.; Xu, K.; Dickson, R. M. Three-Dimensional Single Molecule Rotational Diffusion in Glassy State Polymer Films. *Phys. Rev. Lett.* **2002**, *89* (2), 026101.
(14) Hou, Y.; Higgins, D. A. Single Molecule Studies of Dynamics in Polymer Thin Films and at Surfaces: Effect of Ambient Relative Humidity. *J. Phys. Chem. B* **2002**, *106*, 10306−10315.
(15) Tomczak, N.; Vallée, R. A. L.; van Dijk, E. M. H. P.; Garcia-Parajo, M. F.; Kuipers, L.; van Hulst, N. F.; Vansco, G. J. Probing Polymers with Single Fluorescent Molecules. *Eur. Polym. J.* **2004**, *40* (5), 1001−1011.
(16) Uji-I, H.; Melnikov, S. M.; Deres, A.; Bergamini, G.; Schryver, F. D.; Herrmann, A.; Müllen, K.; Enderlein, J.; Hofkens, J. Visualizing Spatial and Temporal Heterogeneity of Single Molecule Rotational Diffusion in a Glassy Polymer by Defocused Wide-Field Imaging. *Polymer* **2006**, *47* (7), 2511−2518.
(17) Reznik, C.; Darugar, Q.; Wheat, A.; Fulghum, T.; Advincula, R. C.; Landes, C. F. Single Ion Diffusive Transport within a Poly(styrene sulfonate) Polymer Brush Matrix Probed by Fluorescence Correlation Spectroscopy. *J. Phys. Chem. B* **2008**, *112*, 10890−10897.
(18) Wang, S.; Zhu, Y. Molecular Ddiffusion on Surface Tethered Polymer Layers: Coupling of Molecular Thermal Fluctuation and Polymer Chain Dynamics. *Soft Matter* **2010**, *6*, 4661−4665.
(19) Vallée, R. A. L.; Tomczak, N.; Kuipers, L.; Vansco, G. J.; van Hulst, N. F. Single Molecule Lifetime Fluctuations Reveal Segmental Dynamics in Polymers. *Phys. Rev. Lett.* **2003**, *91* (3), 038301.
(20) Reznik, C.; Berg, R.; Foster, E.; Advincula, R.; Landes, C. F. Transient Three-Dimensional Orientation of Molecular Ions in an Ordered Polyelectrolyte Membrane. *J. Phys. Chem. Lett.* **2011**, *2*, 592−598.
(21) Schob, A.; Cichos, F.; Schuster, J.; von Borczyskowski, C. Reorientation and Translation of Individual Dye Molecules in a Polymer Matrix. *Eur. Polym. J.* **2004**, *40* (5), 1019−1026.
(22) Vallée, R. A. L.; Van der Auweraer, M.; Paul, W.; Binder, K. What can be Learned from the Rotational Motion of Single Molecules in a Polymer Melt near the Glass Transition? *Euro. Phys. Lett.* **2007**, *79* (4), 46001.
(23) Flier, B. M. I.; Baier, M. C.; Huber, J.; Müllen, K.; Mecking, S.; Zumbusch, A.; Wöll, D. Heterogeneous Diffusion in Thin Polymer Films As Observed by High-Temperature Single-Molecule Fluorescence Microscopy. *J. Am. Chem. Soc.* **2012**, *134*, 480−488.
(24) Flier, B. M. I.; Baier, M.; Huber, J.; Müllen, K.; Mecking, S.; Zumbusch, A.; Wöll, D. Single Molecule Fluorescence Microscopy Investigations on Heterogeneity of Translational Diffusion in Thin Polymer Films. *Phys. Chem. Chem. Phys.* **2011**, *13* (5), 1770−1775.
(25) Oba, T.; Vacha, M. Relaxation in Thin Polymer Films Mapped across the Film Thickness by Astigmatic Single-Molecule Imaging. *ACS Macro Lett.* **2012**, *1*, 784−788.
(26) Ruiter, A. G. T.; Veerman, J. A.; Garcia-Parajo, M. F.; van Hulst, N. F. Single Molecule Rotational and Translational Diffusion Observed by Near-Field Scanning Optical Microscopy. *J. Phys. Chem. A* **1997**, *101*, 7318−7323.
(27) Tran-Ba, K.-H.; Finley, J. J.; Higgins, D. A.; Ito, T. *J.* Single-Molecule Tracking Studies of Millimeter-Scale Cylindrical Domain Alignment in Polystyrene-Poly(ethylene oxide) Diblock Copolymer Films Induced by Solvent Vapor Penetration. *Phys. Chem. Lett.* **2012**, *3* (15), 1968−1973.
(28) Graves-Abe, T.; Pschenitzka, F.; Jin, H. Z.; Bollman, B.; Sturm, J. C.; Register, R. A. Solvent-Enhanced Dye Diffusion in Polymer Thin Films for Polymer Light-Emitting Diode Application. *J. Appl. Phys.* **2004**, *96* (12), 7154−7163.
(29) Mukherjee, M.; Singh, A.; Daillant, J.; Menelle, A.; Cousin, F. Effect of Solvent-Polymer Interaction in Swelling Dynamics of Ultrathin Polyacrylamide Films: A Neutron and X-ray Reflectivity Study. *Macromolecules* **2007**, *40*, 1073−1080.
(30) Immergut, E. H.; Mark, H. F. Principles of Plasticization. *Adv. Chem. Ser.* **1965**, *48*, 1−26.
(31) Suyatma, N. E.; Tighzert, L.; Copinet, A.; Coma, V. Effects of Hydrophilic Plasticizers on Mechanical, Thermal, and Surface Properties of Chitosan Films. *J. Agric. Food Chem.* **2005**, *53*, 3950−3957.
(32) Erdogan, M.; Özbek, Z.; Çapan, R.; Yagci, Y. Characterization of Polymeric LB Thin Films for Sensor Applications. *J. Appl. Polym. Sci.* **2012**, *123* (4), 2414−2422.
(33) Sitaram, S. P.; Stoffer, J. O.; O'Keefe, T. J. Application of Conducting Polymers in Corrosion Protection. *J. Coating Technol.* **1997**, *69* (866), 65−69.
(34) Liu, F.; Yi, B.; Xing, D.; Yu, J.; Zhang, H. Nafion/PTFE Composite Membranes for Fuel Cell Applications. *J. Membr. Sci.* **2003**, *212* (1−2), 213−223.
(35) Paun, I. A.; Ion, V.; Moldovan, A.; Dinescu, M. Thin Films of Polymer Blends for Controlled Drug Delivery Deposited by Matrix-Assisted Pulsed Laser Evaporation. *Appl. Phys. Lett.* **2010**, *96* (24), 243702−243703.
(36) Chowdhury, A.; Locknar, S. A.; Premvardhan, L. L.; Peteanu, L. A. Effects of Matrix Temperature and Rigidity on the Electronic Properties of Solvatochromic Molecules: Electroabsorption of Coumarin 153. *J. Phys. Chem. A* **1999**, *103*, 9614−9625.
(37) Gorman, J.; Chowdhury, A.; Surtees, J. A.; Shimada, J.; Reichman, D. R.; Alani, E.; Greene, E. C. Dynamic Basis for One-Dimensional DNA Scanning by the Mismatch Repair Complex Msh2-Msh6. *Mol. Cell* **2007**, *28* (3), 359−370.

(38) Ha, T.; Enderle, T.; Chemla, D. S.; Selvin, P. R.; Weiss, S. Quantum Jumps of Single Molecules at Room Temperature. *Chem. Phys. Lett.* **1997**, *271* (1−3), 1−5.
(39) Hou, Y.; Bardo, A. M.; Martinez, C.; Higgins, D. A. Characterization of Molecular Scale Environments in Polymer Films by Single Molecule Spectroscopy. *J. Phys. Chem. B* **2000**, *104*, 212−219.
(40) Fitzpatrick, S.; McCabe, J. F.; Petts, C. R.; Booth, S. W. Effect of Moisture on Polyvinylpyrrolidone in Accelerated Stability Testing. *Int. J. Pharm.* **2002**, *246* (1−2), 143−151.
(41) Bühler, V. *Polyvinylpyrrolidone Excipients for Pharmaceuticals: Povidone, Crospovidone and Copovidone*, 1st ed.; Springer: Berlin, 2005.
(42) Hancock, B. C.; Zografi, G. The Use of Solution Theories for Predicting Water Vapor Absorption by Amorphous Pharmaceutical Solids: A Test of the Flory-Huggins and Vrentas Models. *Pharm. Res.* **1993**, *10* (9), 1262.
(43) Stubberud, L.; Arwidsson, H. G.; Larsson, A.; Graffner, C. Water Solid Interactions II. Effect of Moisture Sorption and Glass Transition Temperature on Compactibility of Microcrystalline Cellulose Alone or in Binary Mixtures with Polyvinyl Pyrrolidone. *Int. J. Pharm.* **1996**, *134* (1−2), 79−88.
(44) Oksanen, C. A.; Zografi, G. The Relationship between the Glass Transition Temperature and Water Vapor Absorption by Polyvinylpyrrolidone. *Pharm. Res.* **1990**, *7* (6), 654−657.
(45) Holman, M. W.; Liu, R.; Zang, L.; Yan, P.; DiBenedetto, S. A.; Bowers, R. D.; Adams, D. M. Studying and Switching Electron Transfer: From the Ensemble to the Single Molecule. *J. Am. Chem. Soc.* **2004**, *126*, 16126−16133.
(46) Dickson, R. M.; Norris, D. J.; Moerner, W. E. Simultaneous Imaging of Individual Molecules Aligned both Parallel and Perpendicular to the Optic Axis. *Phys. Rev. Lett.* **1998**, *81* (24), 5322−5325.
(47) Böhmer, M.; Enderlein, J. Orientation imaging of single molecules by wide-field epifluorescence microscopy. *J. Opt. Soc. Am. B* **2003**, *20* (3), 554−559.
(48) Patra, D.; Gregor, I.; Enderlein, J. Image Analysis of Defocused Single-Molecule Images for Three-Dimensional Molecule Orientation Studies. *J. Phys. Chem. A* **2004**, *108*, 6836−6841.
(49) Layek, A.; De, S.; Thorat, R.; Chowdhury, A. Spectrally Resolved Photoluminescence Imaging of ZnO Nanocrystals at Single-Particle Levels. *J. Phys. Chem. Lett.* **2011**, *2* (11), 1241−1247.
(50) De, S.; Layek, A.; Raja, A.; Kadir, A.; Gokhale, M. R.; Bhattacharya, A.; Dhar, S.; Chowdhury, A. Two Distinct Origins of Highly Localized Luminescent Centers within InGaN/GaN Quantum-Well Light-Emitting Diodes. *Adv. Funct. Mater.* **2011**, *21* (20), 3828−3835.
(51) Rühle, B.; Davies, M.; Lebold, T.; Bräuchle, C.; Bein, T. Highly Oriented Mesoporous Silica Channels Synthesized in Microgrooves and Visualized with Single-Molecule Diffusion. *ACS Nano* **2012**, *6*, 1948−60.
(52) Cheezum, M. K.; Walker, W. F.; Guilford, W. H. Quantitative Comparison of Algorithms for Tracking Single Fluorescent Particles. *Biophys. J.* **2001**, *81* (4), 2378−2388.
(53) Michalet, X. Mean Square Displacement Analysis of Single-Particle Trajectories with Localization Error: Brownian Motion in an Isotropic Medium. *Phys. Rev. E* **2010**, *82*, 041914.
(54) Liao, Y.; Yang, S. K.; Koh, K.; Matzger, A. J.; Biteen, J. S. Heterogeneous Single-Molecule Diffusion in One-, Two-, and Three-Dimensional Microporous Coordination Polymers: Directional, Trapped, and Immobile Guests. *Nano Lett.* **2012**, *12*, 3080−3085.
(55) Qian, H.; Sheetz, M. P.; Elson, E. L. Single Particle Tracking: Analysis of Diffusion and Flow in Two-dimensional Systems. *Biophys. J.* **1991**, *60* (4), 910−921.
(56) Jung, C.; Kirstein, J.; Platschek, B.; Bein, T.; Budde, M.; Frank, I.; Müllen, K.; Michaelis, J.; Bräuchle, C. Diffusion of Oriented Single Molecules with Switchable Mobility in Networks of Long Unidimensional Nanochannels. *J. Am. Chem. Soc.* **2008**, *130*, 1638−1648.
(57) Berg, H. C. *Random Walks in Biology*; Princeton University Press: Princeton, NJ, 1993.
(58) Nelissen, J. M. D. T.; Peters, I. M.; de Grooth, B. G.; van Kooyk, Y.; Figdor, C. G. Dynamic Regulation of Activated Leukocyte Cell Adhesion Molecule−Mediated Homotypic Cell Adhesion through the Actin Cytoskeleton. *Mol. Biol. Cell* **2000**, *11* (6), 2057−2068.
(59) Michalet, X.; Berglund, A. J. Optimal Diffusion Coefficient Estimation in Single-Particle Tracking. *Phys. Rev. E* **2012**, *85*, 061916.
(60) Weber, S. C.; Thompson, M. A.; Moerner, W. E.; Spakowitz, A. J.; Theriot, J. A. Analytical Tools to Distinguish the Effects of Localization Error, Confinement, and Medium Elasticity on the Velocity Autocorrelation Function. *Biophys. J.* **2012**, *102* (11), 2443−2450.
(61) Ernst, D.; Köhler, J. Measuring a Diffusion Coefficient by Single-Particle Tracking: Statistical Analysis of Experimental Mean Squared Displacement Curves. *Phys. Chem. Chem. Phys.* **2013**, *15* (3), 845−849.
(62) Saxton, M. J.; Jacobson, K. Single-Particle Tracking: Applications to Membrane Dynamics. *Annu. Rev. Biophys. Biomol. Struct.* **1997**, *26*, 373−399.
(63) Zheng, Z.; Kuang, F.; Zhao, J. Direct Observation of Rotational Motion of Fluorophores Chemically Attached to Polystyrene in its Thin Films. *Macromolecules* **2010**, *43*, 3165−3168.
(64) Burov, S.; Jeon, J-H; Metzler, R.; Barkai, E. Single Particle Tracking in Systems showing Anomalous Diffusion: The Role of Weak Ergodicity Breaking. *Phys. Chem. Chem. Phys.* **2011**, *13* (5), 1800−1812.
(65) Wang, B.; Anthony, S. M.; Bae, S. C.; Granick, S. Anomalous yet Brownian. *Proc. Natl. Acad. Sci. U.S.A.* **2009**, *106* (36), 15160−15164.
(66) Van Kampen, N. G. *Stochastic Processes in Physics and Chemistry*; North-Holland: Amsterdam, 1992.
(67) Wang, B.; Kuo, J.; Bae, S. C.; Granick, S. When Brownian Diffusion is not Gaussian. *Nat. Mater.* **2012**, *11* (6), 481−485.
(68) Thomas, N. L.; Windle, A. H. A Theory of Case II Diffusion. *Polymer* **1982**, *23* (4), 529−542.
(69) Bronstein, I.; Israel, Y.; Kepten, E.; Mai, S.; Shav-Tal, Y.; Barkai, E.; Garini, Y. Transient Anomalous Diffusion of Telomeres in the Nucleus of Mammalian Cells. *Phys. Rev. Lett.* **2009**, *103* (1), 018102.
(70) Doi, M.; Edwards, S. F. *The Theory of Polymers Dynamics*; Clarendon: Oxford, UK, 1986.
(71) Weber, S. C.; Spakowitz, A. J.; Theriot, J. A. Bacterial Chromosomal Loci Move Subdiffusively through a Viscoelastic Cytoplasm. *Phys. Rev. Lett.* **2010**, *104* (23), 238102.
(72) Elliott, L. C. C.; Barhoum, M.; Harris, J. M.; Bohn, P. W. Single Molecule Tracking Studies of Lower Critical Solution Temperature Transition Behavior in Poly(N-isopropylacrylamide). *Langmuir* **2011**, *27*, 11037−11043.